Early Initiation of Endochondral Ossification of Mouse Femur Cultured in Hydrogel with Different Mechanical Stiffness

Gulsan Ara Sathi, BDS, PhD,[1] Kodai Kenmizaki,[2] Satoshi Yamaguchi, PhD,[3] Hitoshi Nagatsuka, DDS, PhD,[4] Yasuhiro Yoshida, DDS, PhD,[5] Aira Matsugaki, PhD,[2] Takuya Ishimoto, PhD,[2] Satoshi Imazato, DDS, PhD,[3] Takayoshi Nakano, PhD,[2] and Takuya Matsumoto, DDS, PhD[1]

Mineralization is one of the most important processes in normal bone tissue development and in disease condition. Developing a novel and standardized *in vitro* model system that can readily monitor both cellular dynamics and mineralization is crucial for better understanding the bone tissue development and growth. Recent studies indicated that the mechanical environment is a critical condition in mineralization. We hypothesized that hydrogel with different mechanical stiffness can provide a biomimetic mechanical environment that can modulate bone tissue growth and mineralization. A femur of mouse embryo (embryonic day 16) was embedded in agarose hydrogel (2–60 kPa) and cultured in an osteogenic medium for a week. Microcomputed tomography (µCT) results revealed enhanced mineralization was detected in the femur head cultured in the gel condition, whereas no mineralization in the femur head cultured in the control (floating culture) condition. The mineralized region was corresponding to the region of secondary ossification center. Both histological and quantitative analyses indicated that the mineralized region of femur head cultured in 10 kPa gel condition was the highest and the mineralized area was significantly larger than that cultured in 2, 40, and 60 kPa gel condition. Immunofluorescence results indicated the enhanced mineralization caused by the higher chondrogenic differentiation at that region. This enhancement mainly relating to the mechanical forces and not to the oxygen tension was also confirmed. Since this system enhances and shortens the mineralization procedure compared with the conventional two-dimensional or three-dimensional cell culture system, this hydrogel system would be one of the unique models for better understanding the mineralized tissue development.

Introduction

IT IS CRUCIAL to understand mineralization in normal bone tissue development.[1] Mineralization is also important in pathophysiology, such as that for atherosclerosis or rheumatoid diseases.[2] A variety of *in vitro* cell culture systems using osteogenic and chondrogenic cells have been used to investigate mineralization in the cell phase.[3] However, the systems are comparatively different from native biological conditions because the behavior of mineralization-related living cells are highly dynamic and variable in terms of their three-dimensional (3D) structure, mechanical properties, and biochemical microenvironment.[4] Therefore, a novel and standardized *in vitro* model system that can readily monitor both cellular dynamics and mineralization is required.

The mechanical environment is currently perceived as a crucial factor in biological tissue development and growth.[5,6] The migration and proliferation of cells constantly occur during tissue development and growth.[7] Also, cells have a variety of mutual adhesion systems depending on the cell type.[8] Thus, cells are subjected to a variety of internal and external mechanical forces, inducing force-specific signal communications called mechanotransduction. Previous studies have revealed that mechanical stimuli resulting from weight loading and muscle force can modulate bone shape during development and growth.[9,10] Studies have also indicated that the mechanical environment is pivotal in mineralization. For example, cyclic mechanical stimulation induces increased levels of alkaline phosphatase activity, bone-specific protein transcript

[1]Department of Biomaterials, Graduate School of Medicine, Dentistry and Pharmaceutical Sciences, Okayama University, Okayama, Japan.
[2]Division of Materials & Manufacturing Science, Graduate School of Engineering, Osaka University, Osaka, Japan.
[3]Department of Biomaterials, Graduate School of Dentistry, Osaka University, Osaka, Japan.
[4]Department of Oral Pathology and Medicine, Graduate School of Medicine, Dentistry and Pharmaceutical Sciences, Okayama University, Okayama, Japan.
[5]Division of Oral Health Science, Department of Biomaterials and Bioengineering, Graduate School of Dental Medicine, Hokkaido University, Hokkaido, Japan.

levels, and mineralized matrix production in bone marrow stromal cells.[11]

Advancements in biomaterial science have resulted in materials having cellular and tissue biocompatibility. Hydrogel materials have especially attracted a great deal of attention because of their unique biocompatibility, advantageous physical characteristics, and innate structural similarities to the extracellular matrix.[12–14] Previous studies have reported that hydrogels with different mechanical stiffness can potentially manipulate cell fate, including cell proliferation and differentiation.[15,16] For example, when mesenchymal stem cells (MSCs) were cultured on soft substrates, which resembled the stiffness of brain tissue, genetic profiling suggested that these cells underwent neuronal differentiation.[15] In contrast, MSCs on stiff substrates that mimicked bone stiffness underwent osteogenesis.[15] Thus, hydrogel materials are considered to be functional substrates generating a natively mimicked mechanical environment for cells and tissues.

In this study, we hypothesized that hydrogels with different mechanical stiffness could provide a biomimetic mechanical environment that could modulate bone tissue growth, including mineralization. Extracted mouse femur tissues were cultured in agarose hydrogels with different mechanical stiffness to test this hypothesis. We investigated the functional and morphological changes in the cultured tissue, including mineralization and molecular expressions in this study.

Materials and Methods

Physicochemical properties of agarose hydrogel

Different concentrations (0.5–6 wt%) of agarose hydrogel (Lonza) were used. Agarose powder was dissolved in autoclaved distilled water and gel pellets were prepared in a precast polydimethylsiloxane mold with cylindrical holes (Fig. 1). Each hole was 8 mm in diameter and 2 mm in height. The elastic modulus of the fabricated agarose hydrogel was measured using a mechanical testing machine in accordance with Japan Industrial Standards K6503-1996 (JIS: EZ Test; Shimadzu). Briefly, the prepared hydrogel was compressed by using a mechanical tester (Crosshead speed: 1 mm/min). The force value obtained at 2 mm from the gel top after compression was applied to the following equation (Supplementary Data; Supplementary Data are available online at www.liebertpub.com/tec).

$$\text{Young's modulus (Pa)} = \text{force(N)}/\text{surface area (mm}^2)$$

The oxygen tension in the center of gel pellets with different mechanical stiffness was measured using a polarographic oxygen measurement system (IMP-211; Inter Medical). The linear shrinkage of the gel after gelation was measured using the obtained digital camera images of the gel. The gel diameter was measured five times per sample at different orientations with image analysis software (ImageJ; NIH). The diffusion of bovine serum albumin (BSA) protein (2 mg/mL; Thermo Scientific) was analyzed in a modified two-compartment open system to assess the permeability of the hydrogels. The upper compartment was filled with 200 μL of BSA protein. The lower compartment was filled with distilled water. Agarose hydrogel with different concentrations was in the upper compartment placed between the BSA solution and distilled water. The solution from the lower compartment was collected after 24 h and the protein concentration was measured with a microplate reader at 562 nm absorbent points ($n = 4$).

Samples of each gel type were fixed and stained with 1% osmium tetroxide (Sigma-Aldrich) for 2 h for scanning electron microscopy (SEM). The samples were then rapidly frozen and freeze dried under a vacuum. The formed cryogenic gel surfaces were coated with osmium using Neoc-STB (Meiwa-Fosis). Finally, the samples were examined under an acceleration voltage up to 10 kV (DS-720 SEM; Topcon) ($n = 3$).

Isolation and culture of embryonic mice femurs

Femurs were dissected from embryonic day 16 (E16) imprinting control region (ICR) mice (Shimizu Laboratory). Soft tissue, such as adherent muscles and ligaments, was carefully removed. All animal studies were conducted according to the Okayama University's guidelines on the use of laboratory animals (OKU-2013033).

The dissected femurs were placed in the center of a preprepared agarose hydrogel setup (Fig. 1). After gelation, organotypic cultures were incubated in an osteogenic medium (OSM)
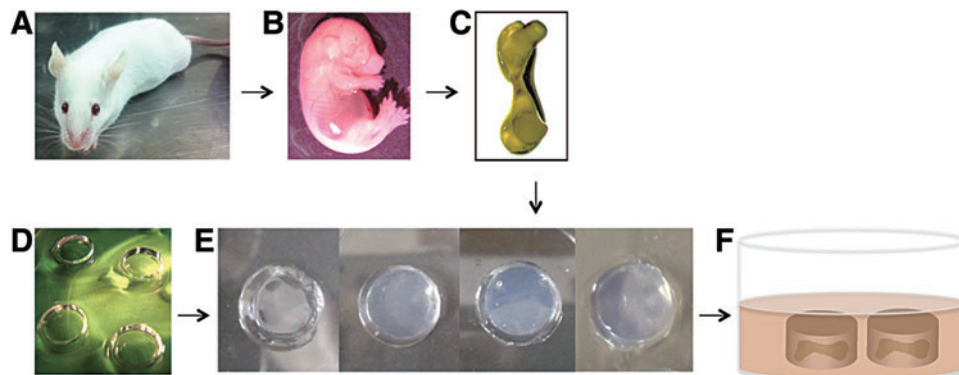

FIG. 1. Experimental outline for embryonic mice femur organotypic culture. **(A)** Imprinting control region pregnant mice were used for this experiment. **(B)** Embryo at embryonic day 16 was taken out and **(C)** femurs were isolated. **(D)** Polydimethylsiloxane mold was used to prepare **(E)** agarose hydrogel with different stiffness. **(F)** Schematic representation of the organotypic culture of embryonic mice femur in hydrogel. Color images available online at www.liebertpub.com/tec

containing an α-Minimum Essential Medium (α-MEM; Wako Pure Chemical), penicillin–streptomycin (10,000 U/mL; Nacalai Tesque), 10% fetal bovine serum (Invitrogen), β-glycerophosphate (1×10^{-2} M; Sigma-Aldrich), L-ascorbic acid (50 mg/mL; Sigma-Aldrich), and dexamethasone (1×10^{-6} M; Sigma-Aldrich) and maintained at 37°C in humidified air with 5% CO_2. The culture media were changed every 2 days for the duration of the experiment up to 7 days ($n = 4$). Femurs cultured under a floating condition were used as a control. The cultured femurs were washed with phosphate buffered saline (Takara Bio) at the end of the experiments and fixed with 4% paraformaldehyde (Wako Pure Chemical).

Microcomputed tomography analysis of femurs

The femurs cultured for 7 days were scanned by using microcomputed tomography (μCT, SMX-100CT-SV; Shimadzu). The X-ray source was set at 29 kV and 27 μA to obtain the best contrast between bone tissues. Reconstructed 3D bone images were analyzed for their macroscopic and microscopic structural properties. The mineralized region of the femur head and the length of the stem were then measured using the image analysis software (ImageJ, NIH).

Histological and immunohistochemical analysis of femurs

The fixed femur samples were dehydrated in a graded series of alcohols and embedded in paraffin. Five-micrometer tissue sections were cut from the femur samples and stained with Hematoxylin–Eosin (HE), 0.5% Alcian Blue 8GX (Waldeck-GmbH) to stain the proteoglycan-rich cartilage matrix, and counterstained with 0.1% Nuclear Fast Red (Waldeck-GmbH). The sections were also stained with Alizarin Red to assess bone mineralization. The femur samples were then analyzed for type I collagen, type II collagen, and sox9 expression. In brief, after microwave or trypsin antigen retrieval and blocking with 1% BSA (Nacalai Tesque) in Tris buffered saline (TBS), the sections were incubated overnight at 4°C with primary antibodies diluted appropriately in TBS containing 1% BSA: either type I collagen (1:600, ab34710; Abcam), type II collagen (1:200, MAB8887; Millipore), or SOX9 (1:300, ab26414; Abcam). Additionally, the expression levels of HIF-1α (1:25; Santa Cruz Biotechnology) and Ki67 (1:1500, ab15580; Abcam) were evaluated in an organotypic culture to determine the hypoxic condition and cell proliferation of femurs during the culture periods. The signal was detected using Alexa Fluor®488 or Alexa Fluor®568-conjugated secondary antibodies (Life Technologies). The images were obtained using a confocal microscope system (C1; Nikon).

Computer simulation

Bone tissue consisting of the bone stem, cartilaginous bonehead, and the attached hydrogel was three-dimensionally modeled with the Finite Element (FE) Method Software (Solid Works Premium 2011). The diameter of the bone tissue was 1.0 mm and the heights of the bone, cartilaginous bonehead, and hydrogel were 2.0, 0.75, and 0.50 mm, respectively. The height of the cartilaginous bonehead varied from 0.75 to 0.95 mm in mimicking tissue growth. The Young's moduli of each component of the bone tissue were as follows: a bone stem of 300 kPa, cartilaginous bonehead of 50 kPa, and hydrogel of 10 or 30 kPa. Poisson's ratio for the entire tissue was 0.30. Compression force was applied to the surface of the hydrogel until it reached the height of the control. The internal displacement within each tissue component was calculated using the Solid Works software. The displacement reflecting the internal force within the tissue was indicated by a color distribution. FE analysis was carried out using a high spec computer (OS: Windows 7 Professional, CPU: Intel Xeon W5590 3.33 GHz, and memory of 24 GB).

Statistical analyses

The statistical analyses of the data included Student's t-test and a one-factor analysis of variance (ANOVA). Scheffe's f-test was used for comparison at a 99% confidence interval. All data points in the graphs represent the mean values and the error bars represent the standard error of the means.

Results

Physicochemical characteristics of agarose hydrogel

Cylindrically shaped agarose gel was fabricated using a polymer mold (Fig. 1). The gel strength altered according to the agarose concentration. The elastic modulus of the prepared agarose gel increased as agarose concentration increased. The elastic moduli of the prepared agarose gel depended on the concentration: they increased from 2, 10, 40, and 60 kPa when the agarose concentration was increased from 0.5 to 6 wt% (Supplementary Fig. S1A). SEM images of 2, 10, 40, and 60 kPa agarose hydrogel revealed an interconnected nanoporous structure with a pore size in the range of 20–40 nm (Supplementary Fig. S1B). The deswelling ratio differed according to the mechanical stiffness of the gel (Supplementary Fig. 2A). However, a permeability test of a different concentrated hydrogel revealed that the protein diffusion rate was real, confined to each gel, and had no significant differences (Supplementary Fig. S2B, C).

Bone tissue cultured in gels with different mechanical stiffness

Femurs were dissected from E16 ICR mice, and cultured in the cylindrically shaped agarose hydrogel with OSM for 7 days (Fig. 1). After the 7-day culture period, no significant differences were observed in the length of the bone stem in any of the organotypic cultured groups (Fig. 2). Dissimilarities were detected in the calcified tissue mass in the femur tissue cultured over 7 days (Fig. 3A). Enhanced mineralization was observed in the femur head cultured in the gel, whereas no mineralization was observed in the femur head cultured under the control condition (floating culture). The mineralized region corresponded to that of the secondary ossification center. The quantitative results indicated that the mineralized region of the femur head cultured in the 10 kPa gel was significantly higher than that cultured in the 2, 40, and 60 kPa gels (Fig. 3B). The proximal head exhibited more enhanced mineralization than the distal head under all conditions (Fig. 3C). The μCT data revealed that
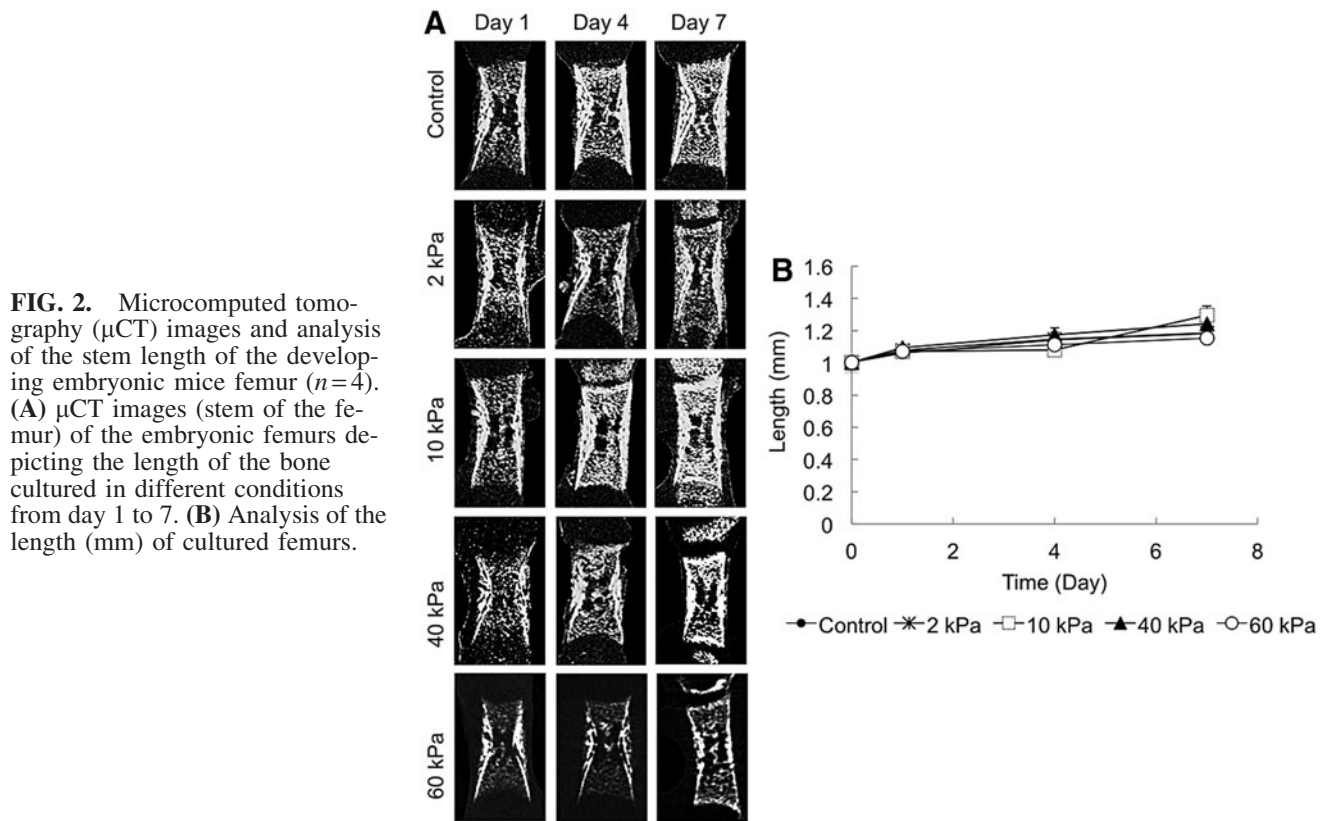
FIG. 2. Microcomputed tomography (μCT) images and analysis of the stem length of the developing embryonic mice femur ($n = 4$). **(A)** μCT images (stem of the femur) of the embryonic femurs depicting the length of the bone cultured in different conditions from day 1 to 7. **(B)** Analysis of the length (mm) of cultured femurs.

there was a very weak or almost negative mineralized region in the 60 kPa gel femur head compared with the others. Therefore, the 60 kPa gel condition was omitted and a further experiment was carried out using the sample cultured under floating (control) and 2–40 kPa gel conditions.

Cell proliferation and differentiation in cultured femur

Biological investigations were carried out to try to understand the mechanism for these phenomena. HE staining indicated that individual cell morphology differed depending on the region in the femur head (Fig. 4A–D). Alizarin Red staining results indicated there was enhanced mineralization of the femur head in the bone tissue cultured in the gel. Further, the mineralization region was markedly larger under the 10 kPa gel condition than that in the other gels (Fig. 4E–H), which was similar to the μCT data. Alcian Blue staining was carried out to determine whether the cells in the femur head exhibited a chondrogenic phenotype. The results indicated that Alcian Blue expanded into a wide region in the femur head cultured in the gel after 7 days, except for the control femur (Fig. 4I–L). The expressions of sox9, type II collagen, and type I collagen staining were assessed to understand the cellular phenotype of the femur head region. The results indicated that the strong expression of sox9 was only in the femur cultured in the 10 kPa gel (Fig. 5A–D). Type II collagen-positive cells were strongly expressed in the inner region of the femur head cultured under all conditions (Fig. 5E–H). Although the tissue exhibited intense mineralized deposition, type I collagen was only positive in the periosteum regions, and not in the femur head (Fig. 5I–L).
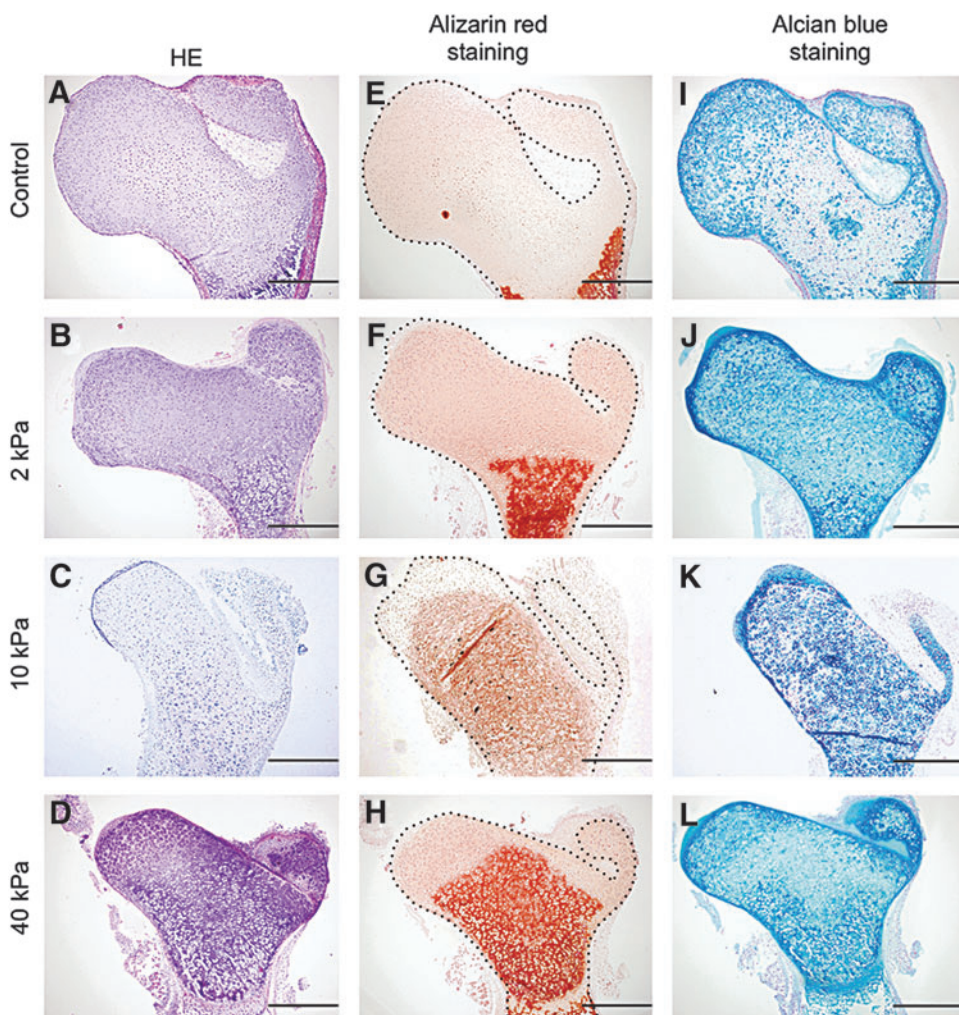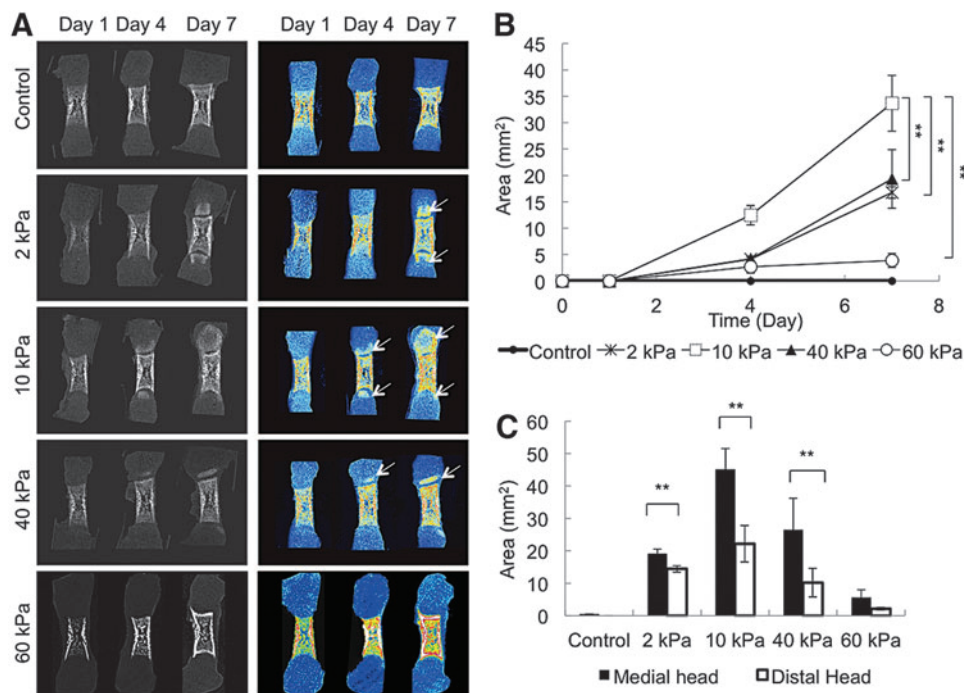
The proliferation of cells in the femur head region was investigated using the cell proliferation marker Ki67 immunostaining. The Ki67-positive cells were most numerous in the femur head cultured in the control. In contrast, fewer Ki67-positive cells were observed in the femur head cultured in the 10 kPa gel (Fig. 6A, B).

Oxygen tension inside gel

Since the tissue was cultured in gels with different mechanical stiffness, the oxygen tension in each gel might have affected cellular behavior in the tissue in the gel. Therefore, the partial oxygen tension (pO$_2$) inside the gel was measured using an oxygen tension tester. The oxygen tension was 16.5%, 15.1%, and 14.5% in 2, 10, and 40 kPa gel, respectively, at the beginning and gradually increased to a normoxic condition during the culture periods (Fig. 7A). Furthermore, HIF-1α immunofluorescence staining was carried out to investigate the effect of the altered oxygen tension on the ischemic reaction. No positive staining was detected in the tissues cultured under gel conditions (Fig. 7B). Thus, it was confirmed that oxygen tension inside gels with different mechanical stiffness hardly affected cell behavior.

Computer simulation

FE analysis of the cultured condition was performed to further understand the mechanical condition in gel. The results indicated that the displacement of tissue was especially in the cartilage region (i.e., femur head region in this study), but not in the bone stem region. The increase in cartilage tissue displacement was calculated
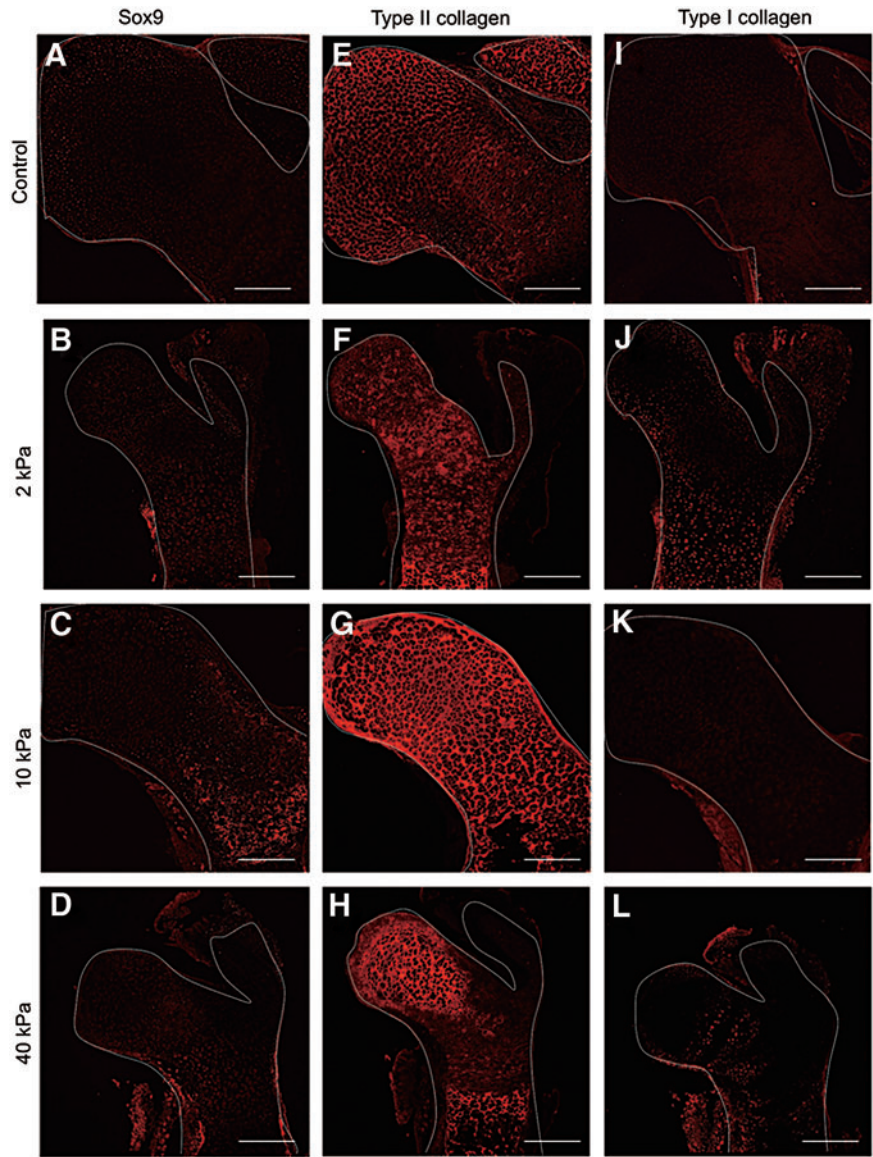
FIG. 3. μCT analysis of organotypic cultured embryonic femurs in control, 2, 10, 40, and 60 kPa conditions ($n = 4$). **(A)** μCT images (whole femur tissue; sagittal sections) of embryonic femurs organotypic cultured in control, 2, 10, 40, and 60 kPa gel conditions up to 7 days. *Arrow* indicates mineralization. **(B)** Graph depicting the total amount of bone formation (mm^2) in both medial and distal regions of the femur. **(C)** Graph showing that medial region contains higher mineralization than distal region. (**$p < 0.001$).

FIG. 4. Histological analysis of the embryonic femurs cultured in the different conditions up to 7 days. This histological analysis was done using **(A–D)** Hematoxylin and Eosin, **(E–H)** Alizarin Red, and **(I–L)** Alcian Blue expression (scale bar = 100 μm).

FIG. 5. Representative images of bone markers sox9 **(A–D)**, type II collagen **(E–H)**, and type I collagen **(I–L)** expression in embryonic mice femur cultured in different hydrogel (scale bar = 100 μm). Color images available online at www.liebertpub.com/tec
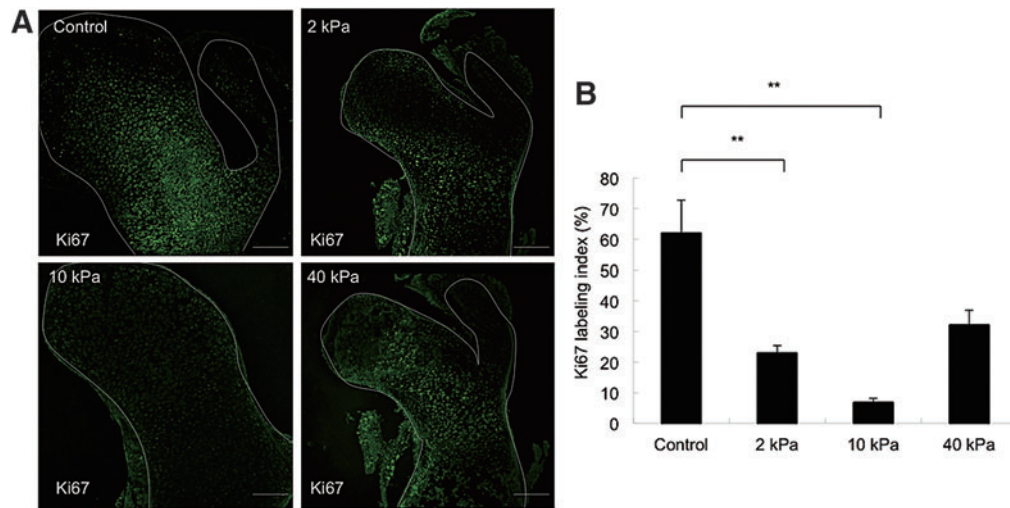

FIG. 6. Representative cases of expression of cell proliferation marker Ki67 in embryonic femur cultured in different gel conditions **(A)** (scale bar = 100 μm). **(B)** Graph represents the Ki67 labeling index (%) (**$p < 0.001$), ($n = 3$). Color images available online at www.liebertpub.com/tec
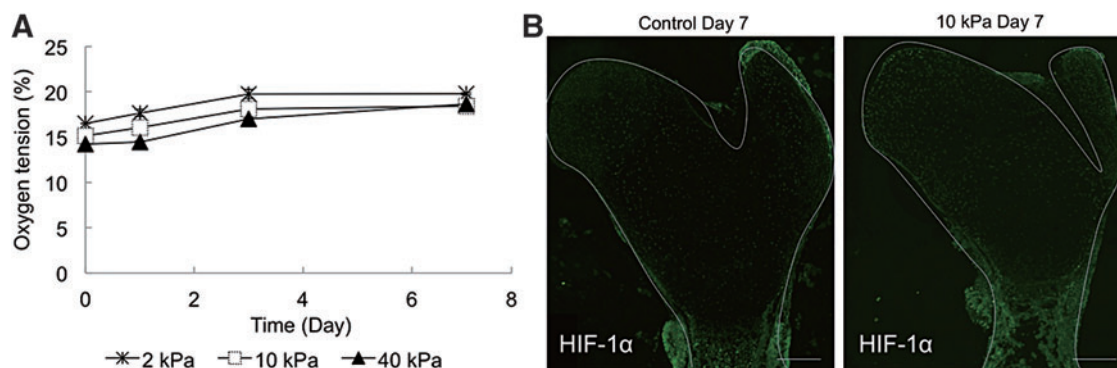
FIG. 7. **(A)** Partial oxygen tension inside the hydrogel during the culturing period ($n = 3$). **(B)** Representative images of HIF-1α expression in embryonic femur cultured in control and 10 kPa gel conditions for 7 days (scale bar = 100 μm). Color images available online at www.liebertpub.com/tec

with an increase in Young's modulus of the attached gel (Supplementary Fig. S3).

Discussion

We built up an *in vitro* system to readily monitor cellular activity during the mineralization process using agarose hydrogels with different mechanical stiffness and applied it to an organotypic bone culture. Agarose, which is a marine algal polysaccharide that forms thermally reversible gels, has been investigated for different applications in tissue engineering and biological studies due to its well-known biocompatibility.[17] Gels in a range of 2–60 kPa were prepared in this study. This range was set on the basis of the Young's modulus of biological tissue (e.g., 1 kPa in embryonic tissue to 60 kPa of immature bone tissue).[15] After a 7-day culture period, the femur head region of bone tissue cultured under the 10 kPa gel condition demonstrated a high intensity of mineralization. It has been reported that optimum mechanical force is responsible for cartilaginous tissue differentiation and promotes mineralization, whereas insufficient or excessive mechanical stimuli can cause tissue degeneration or dystrophic calcification.[18,19] There have also been many reports that have indicated that the osteogenic differentiation of cells is enhanced under stiffer gel conditions. These data were mostly obtained from two-dimensional (2D) culture studies. Cell culture conditions in 3D are somewhat different from 2D conditions. The organotypic culture in the 10 kPa gel exhibited higher mineralization in the femur head region starting from day 4, whereas the femur cultures in the 2 and 40 kPa gels demonstrated mineralization at day 7.

The proximal head revealed more enhanced mineralization than the distal head under all conditions. A recent study has disclosed that there are two distinct development patterns in the medial and the distal region of the femur.[20] The murine distal femur grows a serial sequel of vascular development and establishes a secondary ossification center. In contrast, the proximal femoral epiphysis remains avascular until skeletal maturity, coinciding with chondroepiphyseal ossification.[21] This might be a possible explanation for the higher amount of mineralization in the medial region in this study.

The mechanical environment was recognized as a profound modulating factor for the development, maintenance, and remodeling of bone tissue *in vivo*. Cartilage mechanical conditions favor glycosaminoglycan (GAG) synthesis.[22,23] The amount of GAG, detected with Alcian Blue, increased more in the embryonic femur cultured in the hydrogel than that cultured under the floating condition, confirming that mechanical stiffness with various ranges provoked the chondrocytes to respond in a similar manner. The expressions of different bone and cartilage markers were assessed to understand the cellular phenotype of the femur head region. The results revealed strong expression of type II collagen and sox9 in the femur head region, but type I collagen was almost negative in that area.[24] Therefore, the enhanced mineralization in the femur head cultured in the gel was caused by the promotion of chondrocyte differentiation along with mineralization. These results resemble the initiation of a secondary ossification center during endochondral ossification. The results also revealed fewer Ki67-positive cells in the 10 kPa gel, but more positive cells under the control condition. Previous reports have indicated that cell proliferation and differentiation are opposite in cell fate.[25] Thus, the fewer proliferated cells in the femur head cultured in the 10 kPa gel also support the idea that the cells in this region were in a more differentiated phase.

Recent studies have demonstrated that hypoxia, that is, a condition with low oxygen supply, acts as a strong stimulator for the chondrogenic differentiation of MSCs.[26–29] Therefore, we thought that the enhanced mineralization in the femur head obtained in this study might be related to lower oxygen tension because of the surrounding gel. Interestingly, oxygen tension inside the gel was marginally lower at the beginning, but gradually recovered to the normoxic condition during the culture periods. Since oxygen tension has generally been set below 5% in most hypoxia studies,[26,27] the detected value even under the lowest condition, seemed almost normal in this study. In addition, the expression of HIF-1α, which is an important transcription factor for O_2 homeostasis and is regulated by cellular and tissue oxygen tension,[30–32] was also evaluated. The expression of HIF-1α was almost negative in the femur head region, suggesting that the enhanced mineralization in this study was mainly due to mechanical stimulation by the

surrounding gel, and not because of hypoxia conditions. The tissue cultured in hydrogel is subjected to compressive forces because the surrounding gel becomes a barrier to tissue growth. FE analysis was carried out to confirm this by using a tissue-growing model attached to the gels with different mechanical stiffness. The results indicated that tissue displacement alters, especially in the femur head region, but not in the bone stem region during growth. This also supports the idea that mechanical force enhanced mineralization in the femur head region.

There has been a recent shift in the study of tissue development mechanisms from the use of 2D to the use of 3D culture models that mimic the morphological and functional features of their *in vivo* parental tissues.[33–35] These 3D systems have tremendous potential for bridging the gap between cell-based discovery research and animal models, discovering new therapies, and understanding the development processes.[36] The bone organ culture systems introduced in this study maintained various cells and extracellular matrix interactions and achieved rapid mineralization. Also, a plethora of factors can be added in the hydrogel system to engineer a 3D environment.[37] Thus, this *in vitro* gel-based organ tissue culture system is a promising tool in bone tissue formation and mineralization studies, and even in the ultimate goals for *in vitro* bone tissue synthesis. However, it also needs to be noted that the system should be updated according to the conditions of interest because the gel conditions reproduced in this study were only mechanical stiffness, and not other types of mechanical stimulation (e.g., shear stress caused by flows of blood or body fluids).

Conclusions

An *in vitro* bone tissue culture system within hydrogel was prepared. Rapid mineral deposition was observed within 4 days when the tissue was cultured in a 10 kPa hydrogel. This enhancement was directed by prompt chondrogenic differentiation of the cells at the ends of long bones in an optimal mechanical environment. Since this method of 3D organotypic culture is simple, highly reproducible, and enables monitoring of cellular activity within the tissue, it would be one of the most unique models to better understand the development of mineralized tissue, diseases, and deformities under certain mechanical conditions.

Disclosure Statement

No competing financial interests exist.

References

1. Hall, B.K., and Miyake, T. All for one and one for all: condensations and the initiation of skeletal development. BioEsssays **22,** 138, 2007.

2. Giachelli, C.M. Inducers and inhibitors of bio mineralization: lessons from pathological calcification. Orthod Craniofac Res **8,** 229, 2005.

3. Mackay, A.M., Beck, S.C., Murphy, J.M., Barry, F.P., Chichester, C.O., and Pittenger, M.F. Chondrogenic differentiation of cultured human mesenchymal stem cells from marrow. Tissue Eng **4,** 415, 1998.

4. Lutolf, M.P., and Hubbell, J.A. Synthetic biomaterials as instructive extracellular microenvironments for morphogenesis in tissue engineering. Nat Biotechnol **23,** 47, 2005.

5. Frost, H.M. Wolff's Law and bone's structural adaptations to mechanical usage: an overview for clinicians. Angle Orthod **64,** 175, 1994.

6. Huiskes, R., Ruimerman, R., van Lenthe G.H., and Janssen, J.D. Effects of mechanical forces on maintenance and adaptation of form in trabecular bone. Nature **405,** 704, 2000.

7. Ingber, D.E. Cellular mechanotransduction: putting all the pieces together again. FASEB J **20,** 811, 2006.

8. Campàs, O., Mammoto, T., Hasso, S., Sperling, R.A., O'Connell, D., Bischof, A.G., Maas, R., Weitz, D.A., Mahadevan, L., and Ingber, D.E. Quantifying cell-generated mechanical forces within living embryonic tissues. Nat Methods **11,** 183, 2014.

9. Reich, A., Jaffe, N., Tong, A., Lavelin, I., Genina, O., Pines, M., Sklan, D., Nussinovitch, A., and Monsonego-Ornan, E. Weight loading young chicks inhibits bone elongation and promotes growth plate ossification and vascularization. J Appl Physiol **98,** 2381, 2005.

10. Sharir, A., Stern, T., Rot, C., Shahar R., and Zelzer, E. Muscle force regulates bone shaping for optimal load-bearing capacity during embryogenesis. Development **138,** 3247, 2011.

11. Mauney, J.R., Sjostorm, S., Blumberg, J., Horan, R., O'Leary, J.P., Vunjak-Novakovic, G., Volloch, V., and Kaplan, D.L. Mechanical stimulation promotes osteogenic differentiation of human bone marrow stromal cells on 3-D partially demineralized bone scaffolds *in vitro*. Calcif Tissue Int **74,** 458, 2004.

12. West, E.R., Xu, M., Woodruff, T.K., and Shea, L.D. Physical properties of alginate hydrogels and their effects on *in vitro* follicle development. Biomaterials **28,** 4439, 2007.

13. Stile, R.A., and Healy, K.E. Thermo-responsive peptide-modified hydrogels for tissue regeneration. Biomacromolecules **2,** 185, 2001.

14. Tabata, Y., Miyao, M., Inamoto, T., Ishii, T., Hirano, Y., Yamaoki Y., and Ikada, Y. *De novo* formation of adipose tissue by controlled release of basic fibroblast growth factor. Tissue Eng **6,** 279, 2000.

15. Engler, A.J., Sen, S., Sweeney H.L., and Discher, D.E. Matrix elasticity directs stem cell lineage specification. Cell **126,** 677, 2006.

16. Kong, H.J., Liu, J., Riddle, K., Matsumoto, T., Leach K., and Mooney, D.J. Non-viral gene delivery regulated by stiffness of cell adhesion substrates. Nat Mater **4,** 460, 2005.

17. Watanabe, J., Kashii, M., Hirao, M., Oka, K., Sugamoto, K., Yoshikawa, H., and Akashi, M. Quick-forming hydroxyapatite/agarose gel composites induce bone regeneration. J Biomed Mater Res A **83,** 845, 2007.

18. Brandt, K.D., Myers, S.L., Burr D., and Albrecht, M. Osteoarthritic changes in canine articular cartilage, subchondral bone, and synovium fifty-four months after transection of the anterior cruciate ligament. Arthritis Rheum **34,** 1560, 1991.

19. LeRoux, M.A., Arokoski, J., Vail, T.P., Guilak, F., Hyttinen, M.M., Kiviranta, I., and Setton, L.A. Simultaneous

changes in the mechanical properties, quantitative collagen organization, and proteoglycan concentration of articular cartilage following canine meniscectomy. J Orthop Res **18,** 383, 2000.

20. Cole, H.A., Yuasa, M., Hawley, G., Cates, J.M., Nyman, J.S., and Schoenecker, J.G. Differential development of the distal and proximal femoral epiphysis and physis in mice. Bone **52,** 337, 2013.

21. Kisiday, J.D., Frisbie, D.D., McIlwraith, C.W., and Grodzinsky, A.J. Dynamic compression stimulates proteoglycan synthesis by mesenchymal stem cells in the absence of chondrogenic cytokines. Tissue Eng Part A **15,** 2817, 2009.

22. Burton-Wurster, N., Vernier-Singer, M., Farquhar, T., and Lust, G. Effect of compressive loading and unloading on the synthesis of total protein, proteoglycan, and fibronectin by canine cartilage explants. J Orthop Res **11,** 717, 1993.

23. Bell, D.M., Leung, K.K., Wheatley, S.C., Ng, L.J., Zhou, S., Ling, K.W., Sham, M.H., Koopman, P., Tam, P.P., and Cheah, K.S. SOX9 directly regulates the type-II collagen gene. Nat Genet **16,** 174, 1997.

24. Zhu, L., and Skoultchi, A.I. Coordinating cell proliferation and differentiation. Curr Opin Genet Dev **11,** 91, 2001.

25. Schipani, E., Ryan, H.E., Didrickson, S., Kobayashi, T., Knight, M., and Johnson, R.S. Hypoxia in cartilage: HIF-1alpha is essential for chondrocyte growth arrest and survival. Genes Dev **15,** 2865, 2001.

26. Xu, Y., Malladi, P., Chiou, M., Bekerman, E., Giaccia, A.J., and Longaker, M.T. *In vitro* expansion of adipose-derived adult stromal cells in hypoxia enhances early chondrogenesis. Tissue Eng **13,** 2981, 2007.

27. Kanichai, M., Ferguson, D., Prendergast, P.J., and Campbell, V.A. Hypoxia promotes chondrogenesis in rat mesenchymal stem cells: a role for AKT and hypoxia-inducible factor (HIF)-1alpha. J Cell Physiol **216,** 708, 2008.

28. Malladi, P., Xu, Y., Chiou, M., Giaccia, A.J., and Longaker, M.T. Effect of reduced oxygen tension on chondrogenesis and osteogenesis in adipose-derived mesenchymal cells. Am J Physiol Cell Physiol **290,** C1139, 2006.

29. Hirao, M., Tamai, N., Tsumaki, N., Yoshikawa, H., and Myoui, A. Oxygen tension regulates chondrocyte differentiation and function during endochondral ossification. J Biol Chem **281,** 31079, 2006.

30. Wang, G.L., Jiang, B.H., Rue, E.A., and Semenza, G.L. Hypoxia-inducible factor 1 is a basic-helix-loop-helix-PAS heterodimer regulated by cellular O2 tension. Proc Natl Acad Sci U S A **92,** 5510, 1995.

31. Iyer, N.V., Kotch, L.E., Agani, F., Leung, S.W., Laughner, E., Wenger, R.H., Gassmann, M., Gearhart, J.D., Lawler, A.M., Yu, A.Y., and Semenza, G.L. Cellular and developmental control of O2 homeostasis by hypoxia-inducible factor 1 alpha. Genes Dev **12,** 149, 1998.

32. Wang, H., Flach, H., Onizawa, M., Wei, L., McManus, M.T., and Weiss, A. Negative regulation of Hif1a expression and TH17 differentiation by the hypoxia-regulated microRNA miR-210. Nat Immunol **15,** 393, 2014.

33. Matsumoto, T., Yung, Y.C., Fischbach, C., Kong, H.J., Nakaoka, R., and Mooney, D.J. Mechanical strain regulates endothelial cell patterning *in vitro*. Tissue Eng **13,** 207, 2007.

34. Matsumoto, T., Sasaki, J., Alsberg, E., Egusa, H., Yatani, H., and Sohmura, T. Three-dimensional cell and tissue patterning in a strained fibrin gel system. PLoS One **2,** e1211, 2007.

35. Fischbach, C., Chen, R., Matsumoto, T., Schmelzle, T., Brugge, J.S., Polverini, P.J., and Mooney, D.J. Engineering tumors with 3D scaffolds. Nat Methods **4,** 855, 2007.

36. Miyajima, H., Matsumoto, T., Sakai, T., Yamaguchi, S., An, S.H., Abe, M., Wakisaka, S., Lee, K.Y., Egusa, H., and Imazato, S. Hydrogel-based biomimetic environment for *in vitro* modulation of branching morphogenesis. Biomaterials **32,** 6754, 2011.

37. Sasaki, J., Matsumoto, T., Egusa, H., Matsusaki, M., Nishiguchi, A., Nakano, T., Akashi, M., Imazato, S., and Yatani, H. *In vitro* reproduction of endochondral ossification using a 3D mesenchymal stem cell construct. Integr Biol **4,** 1207, 2012.

Address correspondence to:
Takuya Matsumoto, DDS, PhD
Department of Biomaterials
Graduate School of Medicine, Dentistry
and Pharmaceutical Sciences
Okayama University
2-5-1 Shikata-Cho
Okayama 700-8558
Japan

E-mail: tmatsu@md.okayama-u.ac.jp